SANDIA REPORT

SAND97-8234 • UC–406
Unlimited Release
Printed February 1997

Mixed-Convective, Conjugate Heat Transfer During Molten Salt Quenching of Small Parts

D. R. Chenoweth

Prepared by
Sandia National Laboratories
Albuquerque, New Mexico 87185 and Livermore, California 94551
for the United States Department of Energy
under Contract DE-AC04-94AL85000

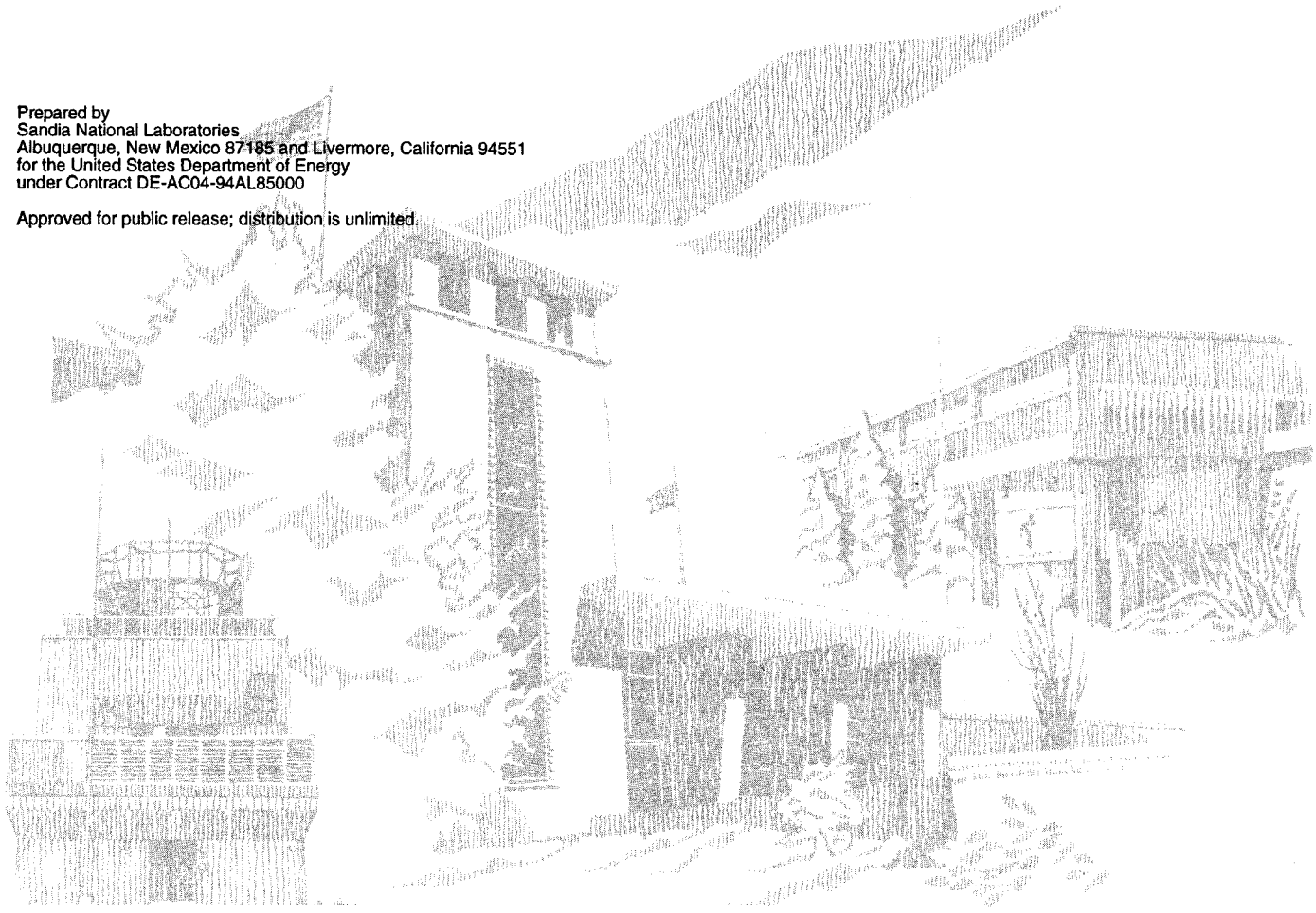

SF2900Q(8-81)

SAND97-8234 UC-406
Unlimited Release
Printed February 1997

Mixed-Convective, Conjugate Heat Transfer during Molten Salt Quenching of Small Parts

D. R. Chenoweth
Sandia National Laboratories

SUMMARY

It is common in free quenching immersion heat treatment calculations to locally apply constant or surface-averaged heat-transfer coefficients obtained from either free or forced steady convection over simple shapes with small temperature differences from the ambient fluid. This procedure avoids the solution of highly transient, non-Boussinesq conjugate heat transfer problems which often involve mixed convection, but it leaves great uncertainty about the general adequacy of the results. In this paper we demonstrate for small parts (dimensions of the order of inches rather than feet) quenched in molten salt, that it is feasible to calculate such non-uniform surface heat transfer from first principles without adjustable empirical parameters. We use literature physical property salt data from the separate publications of Kirst et al., Nissen, Carling, and Teja, et al. for T<1000 F, and then extrapolate it to the initial part temperature. The reported thermal/chemical breakdown of $NaNO_2$ for T>800 F is not considered to be important due to the short time the surface temperature exceeds that value for small parts. Similarly, for small parts, the local Reynolds and Rayleigh numbers are below the corresponding critical values for most if not all of the quench, so that we see no evidence of the existence of significant turbulence effects, only some large scale unsteadiness for brief periods. The experimental data comparisions from the open literature include some probe cooling-rate results of Foreman, as well as some cylinder thermal histories of Howes.

CONTENTS

LIST OF FIGURES

INTRODUCTION

Most of the work described in this report was performed while the author was a member of the heat transfer task team associated with the NCMS CRADA that is concerned with the heat treatment and distortion of gears (NCMS Project # 14-0302). Much of this material appears in the Proceedings of the 2nd International Conference on Quenching and Control of Distortion held in Cleveland, Ohio, November 4-7, 1996.

The quenching of a high temperature material by bringing it into contact with another much lower temperature material (gas,liquid or solid) in order to obtain some desired material properties is a very old and broadly studied subject. Several books (e.g. Liscic et al. (1992)) address the many very complex ramifications and diverse aspects of the widely varied applications encountered when this seemingly simple concept is put to use. We will be concerned here with a very small part of the overall problem.

Here we investigate the numerical prediction of temperatures and cooling rates at various locations in simple cylindrical parts; they are immersed with a vertical axis of symmetry into molten salt quenchants which initially may be nearly stagnant or vigorously agitated by impellers to produce an upward vertical quenchant flow. Among the vast number of liquid quenchants including water, brine, water-soluble polymers, and many natural and synthetic oils with various property modifying additives (Liscic et al.(1992),Skidmore (1986), and Segerberg (1988)), most involve a phase change; therefore, the vapor phase must be accounted for during a vapor blanket stage as well as during the subsequent nucleate boiling regime, both of which occur prior to the convective (forced/free) cooling stage. The molten salt quenchants investigated here primarily involve forced and free convection of a single liquid phase. The CFD and heat transfer empiricism required to describe phase changes and the related multi-phase flow is not necessary; this allows more attention to be paid to the other aspects of the problem before the very difficult two-phase heat-transfer problem is included. Fortunately, there is already adequate experimental data reported in the open literature for the quenching of simple cylindrical shapes in molten salt. We use the data of Howes (1959), Skidmore (1986), and Foreman (1992) to validate our computational capabilities for such quenching applications. We present only temperature and cooling rate information because these can be directly compared to the experimental data. The heat flux heat transfer coefficients and Nusselt number were also produced at every surface/grid line intersection, but a more elaborate analysis is required before that information is presented.

COMPUTATIONAL METHODS

The computational methods utilized to predict the quenching behavior of SS probes and vertical cylinders were developed during the late 1970's and early 1980's; they are embodied in a time-dependent, two-dimensional code, TRACE2D. This code solves the fully non-Boussinesq equations (variable physical properties) using direct Poisson solvers based on modified elliptic solvers of Adams,et al.(1981).

TRACE2D also utilizes an independent variable transformation to a non-physical computational plane, where the calculations are performed using uniform finite-difference meshes, Chenoweth and Paolucci (1981), Paolucci and Chenoweth (1982). However in the physical plane, these grid points can have a highly non-uniform spacial distribution near part surfaces which can be adapted towards a uniform distribution as time evolves. This is done using thermal gradients at the part surface to control the adaption process, and assure that these gradients are accurately

resolved at early time where they are largest. This procedure has allowed TRACE2D to be modified to describe parts of simple shape (arbitrary aspect ratio cylinders and rings) which are placed in motion vertically to simulate actual immersion processes.

TRACE2D has also been generalized to include conjugate heat transfer between finite solid parts and a surrounding liquid quenchant. Thus the heat-transfer process between the part, where conduction is dominant, and the quenchant, where mixed convection (including arbitrary relative amounts of free and forced convection) may be present, is fully coupled. There are no simplifying assumptions other than acoustic wave filtering in the quenchant flow equations. That is, the compressible Navier-Stokes equations which are solved by TRACE2D are simplified only by the small Mach number approximation. This allows the time-step limitation for numerical stability of explicit finite-difference methods to be greatly enlarged. This is accomplished without any appreciable penalty provided the quenchant velocity squared is always much smaller than the local sound speed squared.

The entire procedure was fully validated using air in the free convection regime in Chenoweth and Paolucci (1985, 1986a, 1986b, 1987), and Paolucci and Chenoweth (1988), for laminar flow, where the Rayleigh number,Ra, remained less than 10^8. It was also validated in the transition region where $10^8 < Ra < 10^{10}$, during which unsteady periodic motion progressed toward fully chaotic motion as turbulent motion was approached, Paolucci and Chenoweth (1989). Finally, TRACE2D was used to predict the effects of fully turbulent motion by Paolucci (1990), where $Ra = 10^{10}$. This validation process is important because it is found that comparable Rayleigh numbers are encountered here, but usually in the mixed convection region where the Reynolds number also plays a key role.

PHYSICAL PROPERTIES

The temperature dependent physical properties for mild steel and stainless steel are obtained from Bogaard and Desai (1994) and Touloukain and Ho (1977), respectively.

Many molten salt quenchants consist of various binary and ternary mixtures of KNO_3, $NaNO_3$ and $NaNO_2$; each of these pure components are not as useful separately due to their relatively high nominal freezing points of 607, 582 and 556K, respectively. Therefore physical properties of the pure components will not be given or discussed here unless the "linear molar mixing rule"(LMMR) has been proven to be valid and useful for mixture property estimates when direct experimental mixture measurements are lacking. Kirst, et al. (1940) showed that the largest single effect obtained by blending these components is the greatly reduced mixture freezing point (e.g. as low as 412K for equal weights of KNO_3 and $NaNO_2$). The other physical properties required for CFD analysis of molten salt quenching include mixture viscosity, density, heat capacity and thermal conductivity and they are not so greatly altered by the mixture content. This observation is, however, based on the apparent existence of substantial experimental data for only two popular blends, one binary and the other ternary. The ternary mixture, Kirst, et al.(1940) was originally sold under the tradename HTS and is now called HITEC (similar to PARTHERM 290) and nominally consists of 53wt% KNO_3, 7wt% $NaNO_3$ and 40wt% $NaNO_2$ with a freezing point of about 416K. This blend's experimental data will be considered representative of all "low operating temperature salts"(LOTS) for lack of any other evidence. The binary mixture is nominally an equimolar (near eutectic) blend of the nitrates KNO_3 and $NaNO_3$, with a melting point of about 495K. This blend is similar to PARTHERM 430, and it will be considered to be representative of all "high operating temperature salts"(HOTS) for lack of any other complete set of mixture data. The HOTS higher temperature range often restricts it to austempering applications,

while the LOTS wider temperature range allows it to be used for both martempering and austempering in many cases.

In spite of the very good early work by Kirst, et al.(1940) and later by Janz,et al.(1979), from a CFD point of view, a number of problems remain with respect to the use of molten salts as quenchants in heat treatment applications. Much of the difficulty appears to stem from the fact that other heat transfer applications than heat treatment have driven much of the molten salt research, and those applications involve a more limited temperature range in most cases. The temperature dependent physical properties are required over the entire range from ambient quenchant temperature up to the initial part surface temperature for CFD analysis of quenching applications. Unfortunately viscosity and density data exist only for $T < 875K$. Worse yet, the experimental data for heat capacity and thermal conductivity is even more limited and generally never exceeds 750K. Until higher temperature data is available, this leaves little choice other than extensive property extrapolations to reach some reasonable estimates near the part surface temperature. Such a procedure requires that great attention be paid to the low temperature data. We will return to this discussion following a brief summary of available physical property molten salt mixture data, because there are also other factors involved.

Viscosity:

Kirst, et al. (1940) give the LOTS viscosity in tabular form for $422 < T(K) < 709$. Nissen (1982) gives the HOTS viscosity for $573 < T(K) < 873$ in the form of a cubic fit in T, which is not suitable for extrapolation to higher T values. Both data sets, however, can be well represented by

$$\mu(\text{poises}) = 0.00457 \exp[(800/T(K))^2] \qquad (1)$$

which can be used to extend to higher temperatures until some data becomes available there. The strongest property temperature dependence (non-Boussinesq behavior) is injected into the CFD results by this viscosity expression. Nissen (1982) detected little effect on viscosity from the addition of up to 40mol% KNO_2 to an equimolar mixture of $NaNO_3$ and KNO_3.

Density:

Kirst, et al. give the LOTS density for $422 < T(K) < 828$ which appears to be nearly linear in T and well described by

$$\rho(g/cm^3) = 2.283 - 0.000715\ T(K), \qquad (2)$$

while Nissen (1982) gives the HOTS density as

$$\rho(g/cm^3) = 2.264 - 0.000636\ T(K). \qquad (3)$$

Although very similar, these results do show that apparently the coefficient of thermal expansion $\beta = -(d\rho/dT)/\rho$ is substantially greater for LOTS than for the HOTS mixture. Nissen (1982) shows that the addition of up to 40mol% KNO_2 to an equimolar mixture of the nitrates primarily alters the intercept, and has little effect on the slope or the coefficient of T.

Heat Capacity:

Kirst, et al. give the LOTS heat capacity to be about constant, Cp = 0.373 cal/g K. Using a LMMR, the values of 0.333 cal/g K for KNO_3 and 0.399 cal/g K for $NaNO_3$, obtained by Carling (1983) and Takahashi, et al.(1988) in a narrow T range following their melting, are consistent with this LOTS mixture value provided Cp = 0.405 cal/g K for $NaNO_2$. This value is in good agreement with Janz and Truong (1983) who reported it decreasing from 0.414 to 0.409 as T increased from 570 to 670K. Furthermore the LMMR predicts 0.366 cal/g K for the HOTS heat capacity. The larger T range used by Carling also showed some decrease in Cp with increasing T, especially for T > 650-750K, a region not covered by Takahashi, et al. Such a temperature dependence would be consistent with the suggestion by Tufeu, et al.(1985), that Cp can be estimated for all sodium and potassium nitrates and nitrites using a nearly constant thermal diffusivity

$$\alpha = k/\rho Cp = 0.0016 \text{ cm}^2/\text{sec}.$$

Thus decreasing Cp with increasing T would be true only if the thermal conductivity, k, has a negative T slope which is greater than that of the density, ρ already given, and provided that $\alpha = k/\rho Cp$ really is about constant. We will return to this estimate of Cp following the discussion of thermal diffusivity and thermal conductivity.

Thermal Diffusivity:

The validity of the procedure just mentioned is difficult to prove since it is the T dependence of k and α which has been the most difficult to confirm. Both large positive and negative T slopes have been reported in the literature since 1952. In some cases investigators have in fact assumed constant heat capacity and then used $\alpha = k/\rho Cp$ to infer either k or α behavior from the measurements of the other. During the last two decades it has been reported somewhat consistently that the thermal diffusivity increases with increasing T, while thermal conductivity appears to have a weak decrease with T. These small positive and negative slopes with T for α and k, respectively, have been reported for fairly narrow T ranges. Thus if extrapolated to the part T, they can still represent significant effects.

Neither Kirst, et al. nor Nissen report any thermal diffusivity or conductivity data. Obviously both α and k are not needed for CFD if μ, ρ and Cp are available. However information on both α and k does allow a valuable internal consistency check, especially with respect to T dependence.

Ohta, et al.(1990) show for $NaNO_3$ that α increases from about 0.0014 to 0.0015 cm^2/sec as T increases from 593 to 660K, while for KNO_3 α increases from about 0.0015 to 0.0016 cm^2/sec as T increases from 621 to 694K. Some of the same authors (Otha and Waseda) appear to report data by the same experimental method on the same materials in Waseda, et al.(1992), but with significantly higher magnitudes, 0.0019 to 0.0021 cm^2/sec for both KNO_3 and $NaNO_3$, without explaining the apparent differences. Kato, et al.(1983) find that α is about constant for KNO_3 at about 0.00169 cm^2/sec and similarly for $NaNO_3$ at about 0.00172 cm^2/sec. Odawara, et al.(1977) also report α for $NaNO_3$ to be about constant for $581 < T(K) < 691$, $\alpha = 0.00169$ cm^2/sec, but for LOTS they find that α increases from 0.00168 to 0.00181 cm^2/sec as T increases from 440 to 692K.

$$\alpha(cm^2/sec) = 0.001\ [\ 1.45 + 0.000516\ T(K)\ ] \quad (4)$$

Thermal Conductivity:

Odawara, et al.(1977) also use constant Cp for that thermal diffusivity T range, with density linearly dependent on T, to estimate $k = \alpha\ \rho\ Cp$ for LOTS to be

$$k(w/m/K) = 0.5385 - 0.000047\ T(K) \quad (5)$$

so that had Cp also decreased with T, the very weak T slope of this k would have been strengthened somewhat. Omotani, et al.(1982) used various mixtures of KNO_3 and $NaNO_3$ to establish that thermal conductivity appears to follow a LMMR. For the HOTS (equimolar mixture), a slightly negative T dependence was obtained

$$k(w/m/K) = 0.5461 - 0.000169\ T(K) \quad (6)$$

for $498 < T(K) < 593$. Omotani, et al.(1984) gave a comparable result for the LOTS (ternary mixture)

$$k(w/m/K) = 0.5163 - 0.000038\ T(K) \quad (7)$$

for $427 < T(K) < 584$, showing even weaker dependence on T than for HOTS, similar to that of Odawara, et al.(1977).

The results of Tufeu, et al.(1985) are in substantial agreement with Omotani, et al. for HOTS; however, they obtained a slightly positive T dependence

$$k(w/m/K) = 0.4541 + 0.00058\ T(K) \quad (8)$$

for LOTS.

Kitade, et al.(1989) give results for pure $NaNO_3$ and pure KNO_3 in the narrow T ranges $584 < T(K) < 662$ and $622 < T(K) < 712$, respectively. If these results are combined with a LMMR for the equimolar case,

$$k(w/m/K) = 0.6239 - 0.000265\ T(K) \quad (9)$$

for HOTS.

More recently DiGuilio and Teja (1992) gave similar results for HOTS for $525 < T(K) < 590$,

$$k(w/m/K) = 0.635 - 0.000317\ T(K) \quad (10)$$

which is very similar to the expression just obtained from Kitade, et al. results above. We recommend and use this expression from DiGuilio and Teja results for HOTS (high operating temperature salts) for near equimolar mixtures of KNO_3 and $NaNO_3$. For LOTS (low operating temperature salts) consisting of ternary mixtures similar to HTS(HITEC) we recommend and use the expression (5) which Odawara, et al. estimated from their thermal diffusivity results via a least

squares fit. That expression has coefficients whose percentage increase over the lower values of Omotani, et al. have the same ratio 5.5 as those of DiGuilio and Teja when compared to Omotani, et al. results for HOTS. That is, we are assuming comparable systematic errors for both LOTS and HOTS in the Omotani, et al. results. Therefore, for HOTS, $\alpha = 0.0016$ cm^2/sec, a constant, and

$$Cp(cal/g/K) = k/\alpha\rho = 0.419\ [\ 1.0 - 0.0005\ T(K)\ ]/\ [\ 1.0 - 0.000281\ T(K)\ ] \qquad (11)$$

which decreases about 5% as T increases from 500 to 650K. For LOTS, $Cp(cal/g/K) = k/\alpha\rho = 0.376$, a constant and

$$\alpha(cm^2/sec) = 0.001\ [\ 1.45 + 0.000516\ T(K)\ ] \qquad (12)$$

gives a fully consistent set of physical properties, considering the limited temperature range as well as the considerable scatter in much of the experimental results for k and α.

THERMAL DECOMPOSITION OF QUENCHANT COMPONENTS

It is well known, Kirst, et al.(1940) that LOTS undergoes a thermal decomposition above 700K. In this ternary mixture, it is the nitrite which is most unstable, breaking down to nitrate, oxide and nitrogen gas at a rate which increases with temperature. Fortunately, according to Bradshaw and Meeker (1995), the mixture adjacent to the part surface must remain above this breakdown temperature for periods greater than about a minute, in order for enough decomposition to occur to significantly affect physical properties. Therefore the quenching of small parts is not expected to show the effects of this decomposition, even though larger parts with dimensions of the order of feet would be susceptible to such effects. It is also well known, Nissen (1981), that the nitrates in the HOTS binary mixture breakdown slowly above 800K into nitrites and oxygen gas, among other products. This decomposition is even weaker than the nitrite breakdown in LOTS, so one would also expect it to be unimportant for parts of small dimensions.

MIXED CONVECTION AND TURBULENCE

When both free and forced convection are present, the Richardson number $Ri = Gr/Re^2$ controls much of the flow behavior. Here, $Gr = g\ \beta\ \Delta T\ L^3 / (\mu/\rho)^2$ is the Grashof number, and $Re = \rho\ V\ L / \mu$ is the Reynolds number in terms of the forced convection velocity, V, and the difference between the initial part and ambient quenchant temperature, ΔT. Forced convection is dominant if $Ri << 1$, and free convection is dominant if $Ri >> 1$. For molten salt near ambient temperatures between 450-500K

$$Ri = 225\ L(cm) / V(cm/sec)^2$$

so that $Ri = 1$ implies that the modes of convection have extensive interaction when $V(cm/sec) = 15\ L(cm)^{0.5}$, where L represents a characteristic part dimension. If the combined velocity fields from

immersion and agitation are significantly less than this magnitude, they will not be effective in altering the free convection heat transfer distribution; conversely, if they greatly exceed this value, the results will bear little resemblance to that free convection limit.

Forced Convection:

A forced convection dominated flow, $Ri << 1$, will exhibit laminar boundary layer flow (little wall generated turbulence) in ambient molten salt if

$$Re = 30\ L(cm)\ V(cm/sec) < 10^5.$$

The region $10^5 < Re < 10^6$ is often referred to as the transition region, and fully developed turbulence would usually not occur unless $Re > 10^6$, and enough time elapses at that level in order for it to develop chaotic motion which includes a full spectrum of frequencies and spacial scales. This indicates that for most parts with dimensions less than one foot, there will be little wall generated turbulence when $Ri << 1$ provided $V < 100$ cm/sec, or more generally $V(cm/sec) < 3300 / L(cm)$. Of course even when transition to turbulence does occur, it will occur locally only after the distance along the surface has exceeded the critical value for a given value of velocity. These results are altered somewhat by temperature dependent salt properties as will be discussed briefly below. Also free stream turbulence that is being generated by impellers or other devices is entirely another matter, and it must be included by other means. The forced convection velocity boundary layer thickness, f, grows with distance, s, in the laminar regime like $f(cm) = \sqrt{[s(cm)/V(cm/\sec)]}$ which gives a measure of the spatial resolution required when numerical methods are employed to predict such behavior during quenching. A minimum of 3-5 mesh points are needed inside this boundary layer thickness in order to resolve or describe velocity behavior near the part surface. The thermal boundary layer, which controls the heat flux, can be estimated to be even smaller than that for the velocity by a factor $1/Pr^{0.33}$ when the Prandtl number is greater than unity.

Free Convection:

When the combined effects of agitation and immersion result in $Ri >> 1$, then free convection or buoyant thermal effects control the heat transfer processes. The transition to turbulence is then a much more complex issue. The transition region for vertical surfaces generally occurs for $10^8 < Ra < 5x10^9$, while on upward facing horizontal surfaces it may occur for $3x10^5 < Ra < 10^8$. Extensive downward facing surfaces may never reach a transition region at all unless they are interacting strongly with some adjacent vertical surface. Here the Rayleigh number $Ra = Pr\ Gr$ where $Pr = \mu / \alpha \rho$ is the Prandtl number. In terms of the ambient salt properties, Ra is approximately $Ra = 7000\ \Delta T(K)\ L(cm)^3$ in terms of a charactistic part reference length L and the temperature difference, ΔT, between the initial part and the ambient quenchant values. Thus even for nominal dimensions of a few centimeters, the transition region might be present on the upper portions of the part. Furthermore, the velocity boundary layer thickness is of the order of

$$f(cm) = 0.13\ [\ s(cm) / \Delta T(K)\ ]^{0.25}$$

which grows less rapid with distance along the surface than the forced convection case. Obviously for large temperature differences, this boundary layer can be very thin, so that mesh spacing near the surface can be required to be very small in order to properly resolve the velocity and temperature gradients encountered there during quenching.

Temperature Dependence:

The temperature dependence of the molten salt physical properties, in particular the exponential drop in viscosity with increasing temperature, significantly modifies the picture of transition to turbulence just described. The Prandtl number $Pr = \mu/\alpha\rho$ drops from around 20 to 30 in the ambient salt to around 2 to 3 near the hot part surface early in the quench. Since the Peclet number is $Pe = Pr\ Re$ and the Rayleigh number is $Ra = Pr\ Gr$, one would expect considerable stabilizing influence due to this order of magnitude reduction in viscous effects relative to thermal effects in the thin boundary layer compared to their values outside of that region. Although Ra still increases greatly with increasing T, that increase is much less than that of Gr due to the effect of the large Pr decrease. Similarly, the large increase in Re with increasing T is virtually eliminated by the Pr decrease when Pe is calculated.

This stabilizing effect of a thin layer of much less viscous fluid between a solid wall and a much more viscous fluid is well known; it has been studied for Couette flow by Renardy (1987), and for Poiseuille flow by Pinarbasi and Liakopoulos (1996). It is sometimes referred to as the "thin layer effect" or as "lubrication stabilization" and it can greatly delay transition to turbulence. This same effect can also greatly alter mixed convective behavior, such that a flow which would be turbulent in free convection, can be partially laminarized by the additional influence of forced convection when it is added to the problem, Inagaki (1996) and Jackson, et al.(1994). In fact Kitamura and Inagaki (1987) found that on a vertical heated flat plate with forced upward water flow, the "turbulence suppression" is so great that the mixed convection heat transfer coefficient or Nusselt number can be lowered by as much as 25% compared to that from either pure forced or pure free convection with comparable parameters.

DISCUSSION OF RESULTS

Foreman (1992) gave the center temperature and cooling rate of a 0.25 inch diameter 304SS probe initially at 1600F(1144K) quenched into unagitated dry salt (HOTS) at 495F(531K). Such a small diameter probe can be expected to exhibit a cooling rate which is initially very sensitive to initial conditions, including immersion velocity and depth. Since that information is often not reported, we first use a very slow immersion velocity and compare our calculations quite favorably with the data of Foreman in Figures 1a and 1b, respectively, but the early cooling rate is calculated lower than measured. The early region is expanded on Figure 2, where immersion rate is used as the parameter with the depth arbitrarily selected to be 61 cm. The great sensitivity to immersion rate is shown there, and it appears that the experimental rate probably was between 5 and 15 cm/sec. This sensitivity to immersion history decreases rapidly with increasing probe or cylinder diameter.

Skidmore (1986) gave some Gulf data for the center temperature of a 0.5 inch diameter 18/8SS cylinder with length to diameter ratio of 3. It was initially at 1561F(850C) and was quenched vertically into salt (LOTS) at 427F(220C). Again reasonable agreement between the data and calculation is obtained, but the calculated center temperature is somewhat lower than the data for much of the quench, see Figure 3.

Howes (1959) gave a very wide variety of results for SS cylinders with length to diameter ratio 2 (also some L/D = 1 results) initially at either 800C or 900C quenched vertically into LOTS at a variety of ambient temperatures (150C-400C). The cylinders had diameters of 1, 1.5, 2 and 3 inches. They were quenched into both unagitated and agitated molten salt (estimated vertical

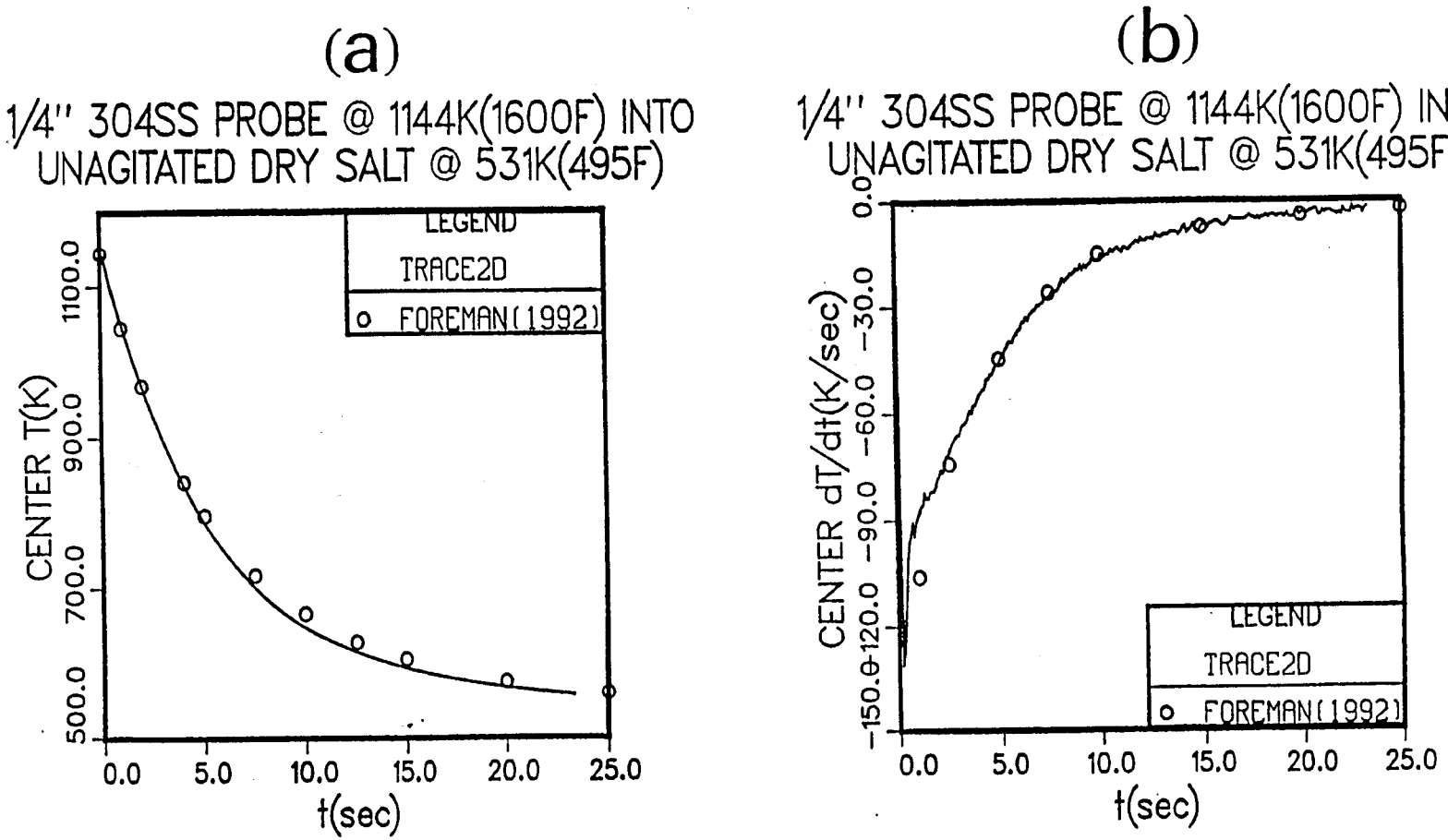

Figures 1a,1b Foreman Quarter Inch SS Probe, Small Immersion Rate

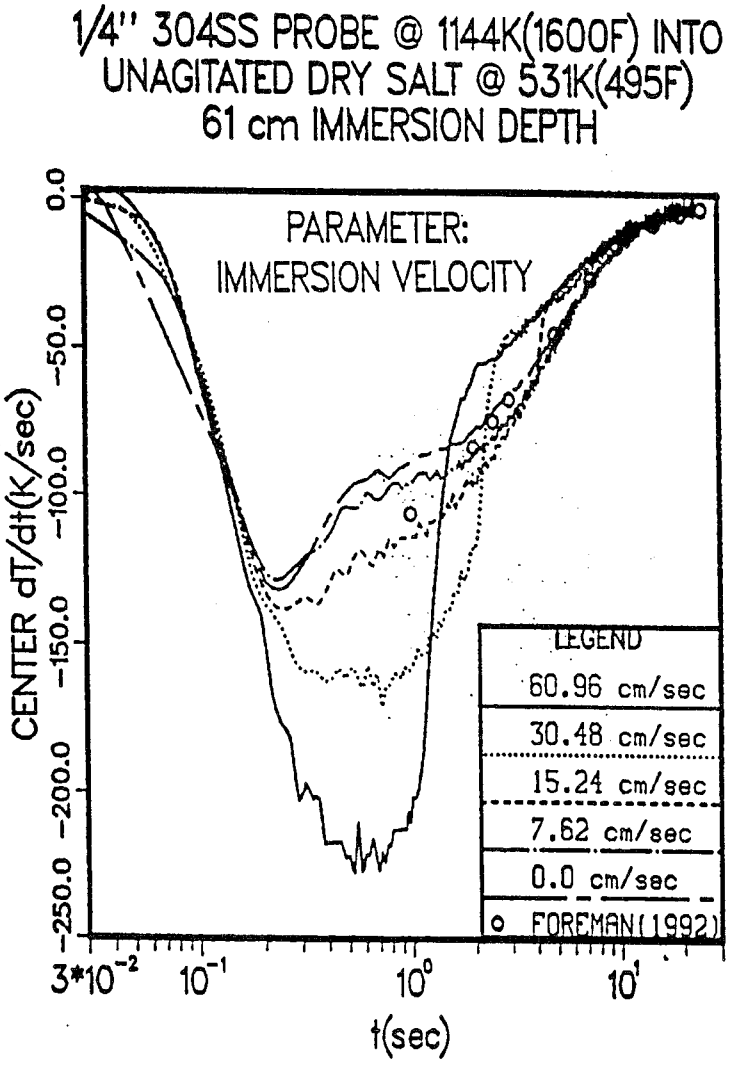

Figure 2 Foreman Quarter Inch SS Probe, Parameter Immersion Rate

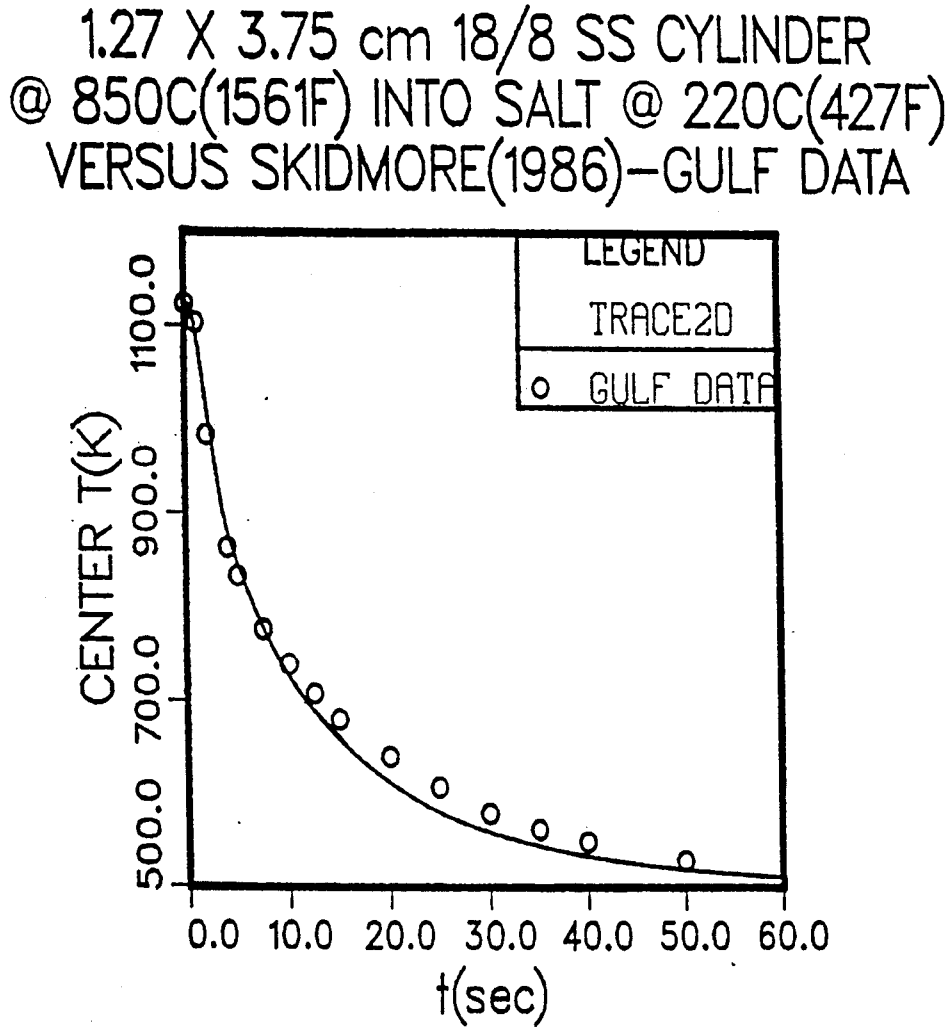

Figure 3 Skidmore/Gulf Half Inch SS Cylinder, L/D = 3

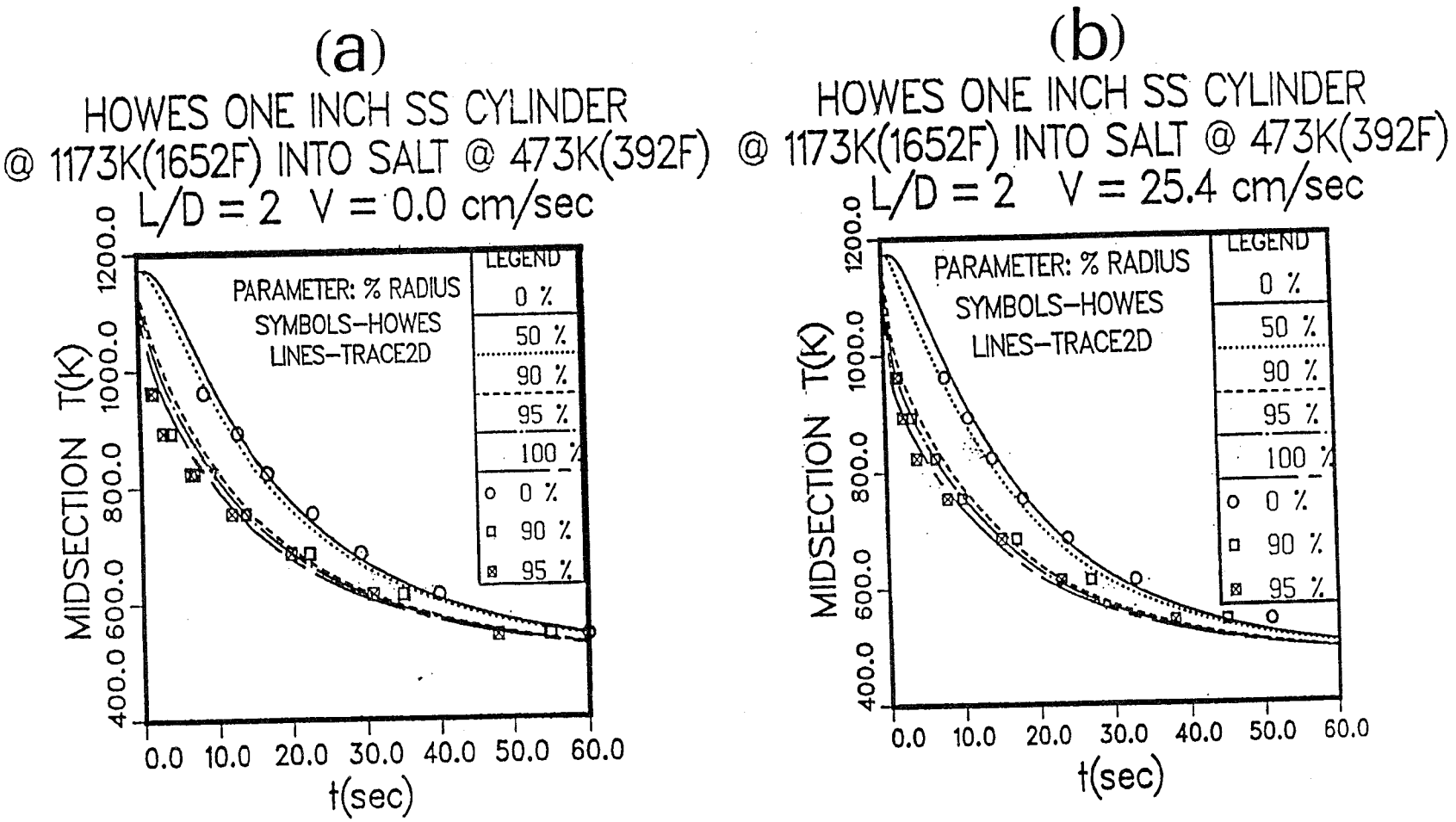

Figures 4a,4b Howes One Inch SS Cylinder, L/D = 2, V = 0.0 and 25.4 cm/sec

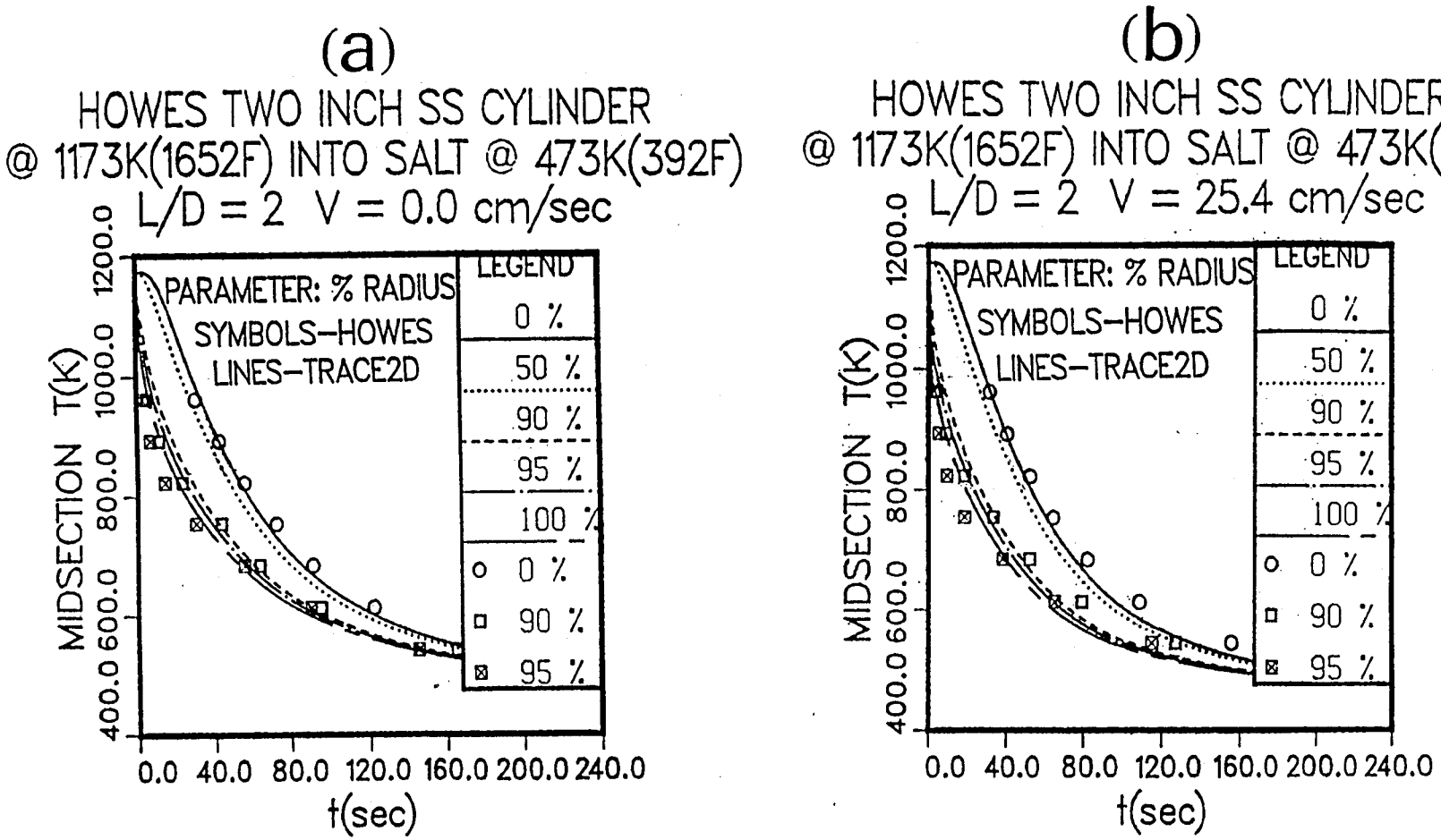

Figures 5a,5b Howes Two Inch SS Cylinder, L/D = 2, V = 0.0 and 25.4 cm/sec

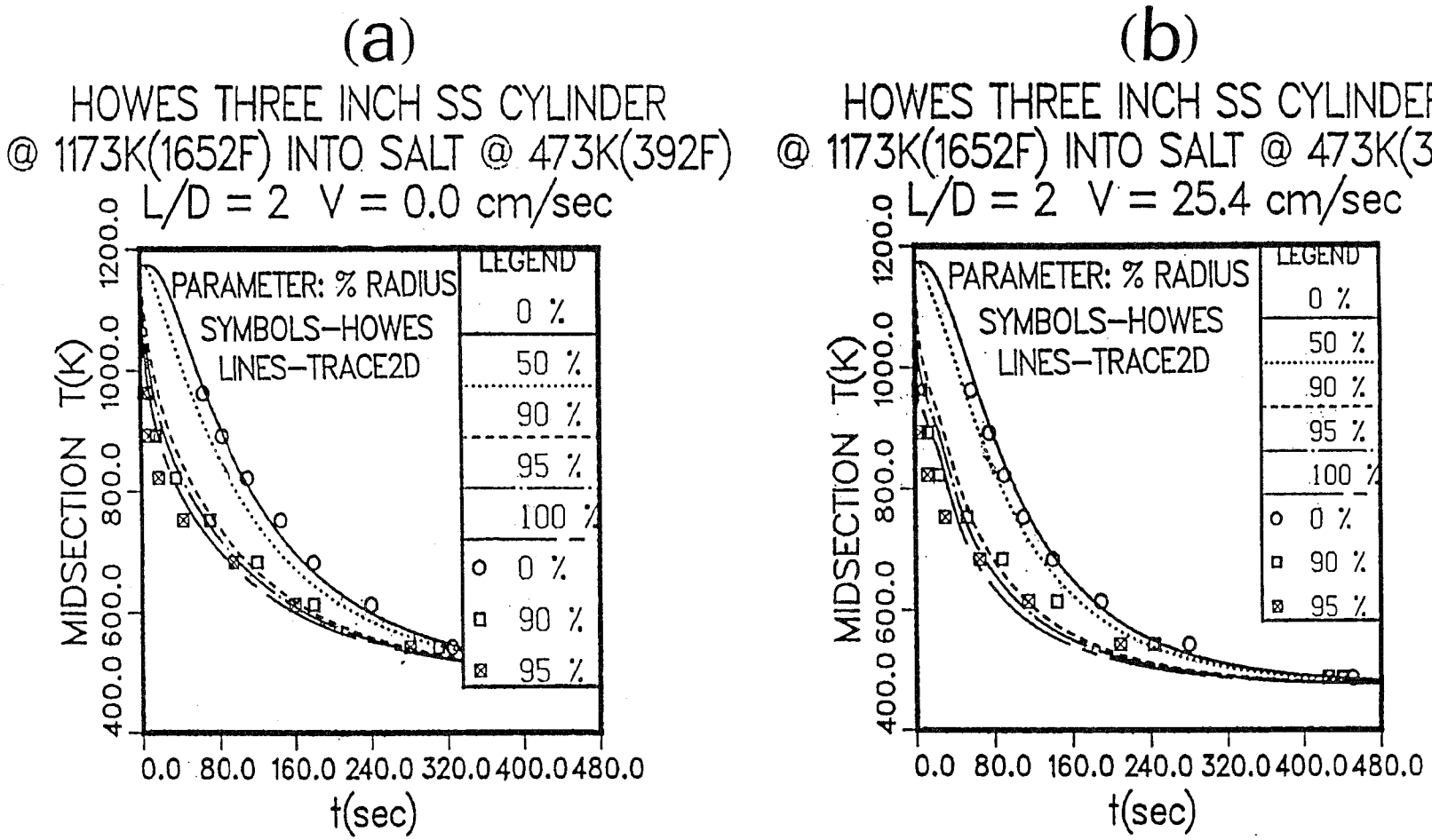

Figures 6a,6b Howes Three Inch SS Cylinder, L/D = 2, V = 0.0 and 25.4 cm/sec

velocity of 25.4 cm/sec). Results from 40 different parameter combinations were given in tabular form for L/D = 2. Temperatures were measured at the cylinder midsection at three different radial positions (0, 90 and 95%). The results calculated with TRACE2D for all diameter cylinders in unagitated salt have similar agreement with the Howes data as shown above for the smaller diameter probes and cylinders. An example is given on Figure 4a for the one inch cylinder with L/D = 2 initially at 1173K quenched into salt at 473K. Here we give 5 calculated radial positions compared to the 3 measured radial positions of Howes. The results show the high thermal gradient near the surface compared to the very low one near the part center. We show results on Figure 4b for the 25.4 cm/sec agitated case involving the one inch cylinder initially at 1173K quenched into salt at 473K. The agitated case shows the expected faster cooling compared to the Figure 4a unagitated case which was identical otherwise. Finally Figures 5 and 6 give similar results for the two and three inch cylinders in both unagitated and agitated salt, showing the expected greatly increased time scales. The calculations still agree well with the data, in spite of the greatly increased Rayleigh numbers for these larger cylinders. This can be explained as was discussed in the Mixed Convection and Turbulence section, by a delayed transition to turbulence due to lubrication stablization in the low viscosity boundary layer.

RELATED PUBLICATIONS IN PREPARATION

This SAND Report is a slightly expanded version of the NCMS paper given at the Second International Conference on Quenching and Control of Distortion held in Cleveland, Ohio, November 4-7, 1996. It contains only temperature and cooling rate at a few locations in some cylinders and probes quenched in molten salt; these were chosen specifically for comparison with existing thermocouple data available in the open literature in order to validate CFD results and procedures. Obviously a great deal more of that information is in our possession for these cases as well as other aspect ratio cylinders; similarly we have analyzed many other cases involving various general rings with a wide variety of aspect ratios and inside to outside diameter ratios. In addition to the local temperature and cooling rate values, the local surface heat flux Q, the related heat transfer coefficient h, and the local Nusselt number Nu were generated versus nondimensional time and spacial coordinates. This information has allowed the development of quite general parameter correlations in terms of the governing nondimensional parameters describing free and forced convection (Ra,Re,Ri) as well as the Prandtl number Pr. Furthermore an exhaustive study of the special behavior and physical content of such elaborate results has allowed approximate analytical solutions to be developed; these give considerable accuracy with very little computational effort, while still retaining essentially all of the pertinent physical characteristics of the quenching phenomena. The generalized quenching correlations as well as the approximate analytical solutions for cylinders and rings are the subject of two additional papers now being prepared for future publication.

All of the quenching results computed to date have relied heavily on the adaptive, nonuniform finite-difference grids; these were alluded to in the computational methods section where the early 1981 version was referenced. As might be expected, many improvements and generalizations have occurred in this area since that time. The seventh version now being prepared for future publication, even allows the part to be placed into motion relative to the salt reservoir, so that actual air to salt immersions and withdrawals can be studied in detail; also it is now possible to prescribe an oscillatory part trajectory while it is in the salt, with different immersion and withdrawal rates as well as varying pauses during direction reversals. This flexibility can be used to partially compensate for the fixed gravitational direction effects. The oscillatory part motion allows the forced convection to alternately interchange the top and bottom of the part to produce more uniform heat

flux distributions when averaged over time. This technique is currently being designed into some modern quench tank systems.

In the mixed convection and turbulence section we briefly described the "lubrication stabilization" and delayed transition effects resulting from an order of magnitude decrease in local Prandtl number as the part surface temperature is approached from the ambient quenchant. It is quite significant that we can numerically predict these results, which were previously obtained by other means in the literature. It is even more remarkable that we can numerically predict the "turbulence suppression" which results in a large reduction in heat transfer in the mixed convection regime relative to pure forced or pure free convection with comparable parameters. This result had been previously reported in the literature only via experimental data. Our numerical capabilities have allowed us to obtain a more general understanding of both of these related phenomena. We expect to document these results in the near future.

A very innovative procedure has recently allowed the third spacial dimension to be added to the current code without disrupting the very efficient numerical solution structure, which uses modified direct Poisson solvers and adaptive nonuniform finite-difference grids, that has been so successful to date. This development has allowed probes, cylinders and rings of arbitrary aspect ratio to be numerically quenched when their axis of symmetry is not aligned with the gravitational vector and/or the forced convection flow direction. These very interesting results are being prepared for publication to show the significant effects which can occur when such nonalignment is present.

Although the calculations given here were for SS parts, the TRACE2D code has long included the thermal effects resulting during the solid part phase change involving the transition from austenite to martensite occurring during quenching of low carbon steels. Such results have already been produced for cylinders and rings and they allow these effects to be discussed in some detail in a future publication.

Finally, the greatest effort and by far the most successful advance in computational modeling with the current substantially modified code has occurred in relation to the quenchant phase changes. This is extremely important because most liquid quenchants do produce a significant vapor phase which results in an early vapor barrier region with greatly reduced heat fluxes; this region is followed by a nucleate boiling region where the maximum heat fluxes occur, prior to the final region where convection phenomena are dominant as was the case for molten salt during the entire quench. The original phenomenological modeling procedure presented to the NCMS working group required major modifications before the current highly successful model was finally validated. The current phase change model involves less empiricism and relies more heavily on first principles than did the original less successful model. To date it has been validated only with water for a wide range of cases. This is true for two reasons. First, water is the quenchant whose liquid and vapor physical properties are best known. Second, the highest quality experimental data existing in the open literature uses water as the quenchant. This model and the related water validation results will be the subject of several important publications which are now being prepared.

REFERENCES

Adams, J. C., Swarztrauber, P. N. and Sweet, R. A., Elliptic Problem Solvers (ed. M. H. Schultz) pp.187-190, Academic Press, 1981.

Bogaard, R. H. and Desai, P. D., Thermal Conductivity, Specific Heat, Thermal Expansion, . . ., HTMIAC Special Report 52, January, 1994.

Bradshaw, R. W. and Meeker, D. E., Private Communication, Material Chemistry Department, Sandia National Laboratory, Livermore, California, 1995.

Carling, R. W., Thermochim. ACTA V60, p.265, 1983.

Chenoweth, D. R. and Paolucci, S., On Optimizing Nonuniform Finite-Difference Grids for Boundary Regions in Transient Transport Problems, Sandia National Laboratories Report, SAND81-8204, February 1981.

Chenoweth, D. R. and Paolucci, S., Phys. Fluids V28, pp. 2365-2374, 1985.

Chenoweth, D. R. and Paolucci, S., J. Fluid Mech. V169, pp.173-210, 1986.

Chenoweth, D. R. and Paolucci, S., Phys. Fluids V29, pp. 3187-3198, 1986.

Chenoweth, D. R. and Paolucci, S., Phys. Fluids V30, pp. 1561-1564, 1987.

DiGuilio, R. M. and Teja, A. S., Int. J. Thermophys. V13, pp.575-592, 1992.

Foreman, R. W., Proc.First Int. Conf. on Quenching and Control of Distortion, (ed.G. E. Totten) pp.87-94, Chicago, Illinois, September 1992.

Howes, M. A. H., The Cooling of Steel Shapes in Molten Salt and Hot Oil, Ph.D. Thesis, London University, 1959.

Inagaki, T., J. Heat Transfer, V118, pp.213-215, 1996.

Jackson, J. D., Axcell, B. P., and Walton, A., Exp. Heat Transfer, V7, pp.71-90, 1994.

Janz, G. J., Allen, C. B., Bansal, N. P., Murphy, R. M. and Tomkins, R. P. T., Physical Properties Data Compilations Relevent to Energy Storage. Part II Molten Salts: Data on Single and Multi-Component Salt Systems, NSRDS-NBS 61, April 1979.

Janz, G. J. and Truong, G. N, J. Chem. Eng. Data,V28, p.201, 1983.

Kato, Y., Furukawa, K., Araki, N., and Kobayasi, K., 8ETPC Proceedings , pp.73-80, High Temperatures-High Pressures V15, pp.191-198, 1983.

Kirst, W. E., Nagle, W. M. and Castner, J. B., Trans. Am. Inst. Chem. Eng.V36, p.371, 1940.

Kitade, S., Kobayashi, Y., Nagasaka, Y. and Nagashima, A., High Temperatures-High Pressures, V21, pp.219-224, 1989.

Kitamura, K. and Inagaki, T., Int. J. Heat Mass Transfer, V30, n1, pp.23-41, 1987.

Liscic, B., Tensi, H. M. and Luty, W., Editors, Theory and Technology of Quenching (a handbook) Springer-Verlag, 1992.

Nissen, D. A., J. Chem. Eng. Data V27, pp.269-273, 1982.

Nissen, D. A., The Chemistry of the Binary $NaNO_3$-KNO_3 System, Sandia National Laboratories, Livermore, California, Report SAND81-8007, June 1981.

Odawara, O., Okada, I., and Kawamura, K., J. Chem. Eng. Data, V22, pp.222-225, 1977.

Ohta, H., Ogura, G., Waseda, Y. and Suzuki, M., Rev. Sci. Instr. V61, pp.2645-49, 1990.

Omotani, T., Nagasaka, Y. and Nagashima, A., Int. J. Thermophys.,V3, pp.17-25, 1982.

Omotani, T. and Nagashima, A., J. Chem. Eng.Data, V29, pp.1-3, 1984.

Paolucci, S. and Chenoweth, D. R., J. Comp. Phys., V47, n3, pp.489-496, September 1982.

Paolucci, S. and Chenoweth, D. R., J. Heat Transfer, V110, pp.625-634, August 1988.

Paolucci, S. and Chenoweth, D. R., J. Fluid Mech. V201, pp.379-410, 1989.

Paolucci, S., J. Fluid Mech. V215, pp.229-262, 1990.

Pinarbasi, A. and Liakopoulos, A., Int. Comm. Heat Mass Transfer, V23, n4, pp.485-493, 1996.

Renardy, Y., Phys. Fluids, V30, n6, pp.1627-37, 1987.

Segerberg, S. O., Heat Treating, pp.30-33, 1988.

Skidmore, C., Heat Treatment of Metals, V2, pp.34-38, 1986.

Takahashi, Y., Sakamoto, R., and Kamimoto, M., Int. J. Thermophys.V9, pp.1081-90, 1988.

Touloukian, Y. S. and Ho, C. Y., Editors, Thermophysical Properties of Selected Aerospace Materials—Part II: Thermophysical Properties of Seven Materials, CINDAS-Purdue University, pp.37-58, 1977.

Tufeu, R., Petitet, J. P., Denielou, L. and Le Neindre, B., Int. J. Thermophys. V6, pp.315-330, 1985.

Waseda, Y., Masuda, M. and Ohta, H., Proc. Fourth Int.Sympos. on Advanced Nuclear Energy Res. pp.298-301, February 5-7, Mito, Wraki, Japan, 1992.

Unlimited Release

8000	MS9001	T. O. Hunter; Attn: J. B. Wright, 2200 (MS9005) M. E. John, 8100 (MS9004) L. A. West, 8200 (MS9420) W. J. McLean, 8300 (MS9054) R. C. Wayne, 8400 (MS9007) P. N. Smith, 8500 (MS9002) P. E. Brewer, 8800 (MS9141) D. L. Crawford, 8900 (MS9003)
8700	MS9405	T. M. Dyer; Attn: M. W. Perra, 8711 (MS9402) M. I. Baskes, 8712 (MS9403) J. C. F. Wang, 8713 (MS9403) G. J. Thomas, 8715 (MS9402) K. L. Wilson, 8716 (MS9161) W. G. Wolfer, 8717 (MS9161) M. R. Birnbaum, 8742 (MS9042) W. A. Kawahara, 8746 (MS9042)
8743	MS9042	D. R. Chenoweth (5)
8743	MS9405	P. E. Nielan
8815	MS9021	Technical Communications Department, 8815/Technical Library, 4414 (MS0899)
8815	MS9021	Technical Communications Department, 8815, for OSTI (2)
4414	MS0899	Technical Library (4)
8940-2	MS9018	Central Technical Files (3)